

CrossMark  
click for updatesCite this: *J. Mater. Chem. A*, 2015, 3, 16279

# Ultra low band gap $\alpha,\beta$ -unsubstituted BODIPY-based copolymer synthesized by palladium catalyzed cross-coupling polymerization for near infrared organic photovoltaics†

Benedetta M. Squeo,<sup>a</sup> Nicola Gasparini,<sup>b</sup> Tayebah Ameri,<sup>b</sup> Alex Palma-Cando,<sup>c</sup> Sybille Allard,<sup>c</sup> Vasilis G. Gregoriou,<sup>ad</sup> Christoph J. Brabec,<sup>be</sup> Ullrich Scherf<sup>c</sup> and Christos L. Chochos<sup>\*a</sup>

A new ultra low band gap (LBG)  $\alpha,\beta$ -unsubstituted BODIPY-based conjugated polymer has been synthesized by conventional cross coupling polymerization techniques (Stille cross coupling) for the first time. The polymer exhibits a panchromatic absorption spectrum ranging from 300 nm to 1100 nm and an optical band gap ( $E_g^{opt}$ ) of 1.15 eV, suitable for near infrared (NIR) organic photovoltaic applications as electron donor. Preliminary power conversion efficiency (PCE) of 1.1% in polymer : [6,6]-phenyl-C<sub>71</sub>-butyric acid methyl ester (PC<sub>71</sub>BM) 1 : 3 weight ratio bulk heterojunction (BHJ) solar cells has been achieved, demonstrating very interesting and promising photovoltaic characteristics, such as good fill factor (FF) and open circuit voltage ( $V_{oc}$ ). These results showing that by the proper chemical design, new  $\alpha,\beta$ -unsubstituted BODIPY-based NIR copolymers can be developed in the future with suitable energy levels matching those of PC<sub>71</sub>BM towards more efficient NIR organic photovoltaics (OPVs).

Received 10th June 2015  
Accepted 10th July 2015

DOI: 10.1039/c5ta04229a

www.rsc.org/MaterialsA

## 1. Introduction

Low band gap (LBG) organic materials that absorb into the near-infrared (NIR) are of great interest in the recent years for a number of potential applications.<sup>1</sup> For example, the use of NIR-absorbing or NIR photovoltaic organic materials (small molecules or polymers) could extend the material's absorption into the NIR spectral region and even beyond 1000 nm wavelength, which in principle could enhance the current power conversion efficiency (PCE) of organic photovoltaics (OPVs).<sup>2</sup>

Even though semiconducting polymers with ultra LBGs have been synthesized before,<sup>3–19</sup> the challenge in designing and synthesizing materials that have a good photoresponse beyond

900 nm and an appreciable PCE in polymer : fullerene solar cells lies (among others) in the precise energy level control that is required. Two major methodologies are employed to fine tune the band gap and energy level alignment of conjugated polymers. One methodology relies on the donor–acceptor (D–A) approach and the other on the stabilization of the quinoid structure.<sup>20</sup> D–A approach is the most common tool to synthesize NIR conjugated polymers due to the plethora of functional electron rich and electron deficient building blocks. In order to develop ultra LBG D–A polymers, usually strong electron rich units and strong electron deficient building blocks are used. Common monomer units function as strong electron donors include pyrrole, thiophene, ethylenedioxythiophene (EDOT), bridged bithiophenes derivatives *etc.*<sup>21</sup> Moreover, the most well-known strong electron deficient units used to construct NIR D–A polymers are diketopyrrolopyrrole dyes,<sup>4c,13a,14c</sup> benzobisthiadiazole,<sup>3a,3g</sup> pyrazinoquinoxaline derivatives,<sup>9b,10a</sup> thiadiazoloquinoxaline derivatives,<sup>10a,11b,c</sup> annelated benzotriazole,<sup>10b</sup> thienoisindigo,<sup>4b,13b</sup> emreladicene,<sup>3f</sup> cyclopentadithiophenone,<sup>14a</sup> tetraaza-benzodifluoranthene diimides,<sup>8a–c</sup> *etc.*<sup>3g,22</sup>

One of the less explored electron deficient monomers for the synthesis of NIR conjugated polymers is the so-called, 4,4-difluoro-4-bora-3a,4a-diaza-s-indacene, commonly known as BODIPY (Scheme 1).<sup>23</sup> BODIPY dyes were first discovered in 1968 by Treibs and Kreuzer<sup>24</sup> and exhibit unique properties such as large absorption coefficients, high fluorescence quantum yields, and remarkable photostability.<sup>23</sup> In addition,

<sup>a</sup>Advent Technologies SA, Patras Science Park, Stadiou Street, Platani-Rio, 26504 Patra, Greece. E-mail: cchochos@advent-energy.com

<sup>b</sup>Institute of Materials for Electronics and Energy Technology (I-MEET), Friedrich-Alexander-University Erlangen-Nuremberg, Martensstraße 7, 91058 Erlangen, Germany

<sup>c</sup>Macromolecular Chemistry Group (buwmakro) and Institute for Polymer Technology, Bergische Universität Wuppertal, Gaußstraße 20, D-42119 Wuppertal, Germany

<sup>d</sup>National Hellenic Research Foundation (NHRF), 48 Vassileos Constantinou Avenue 11635, Athens, Greece

<sup>e</sup>Bavarian Center for Applied Energy Research (ZAE Bayern), Haberstrasse 2a, 91058 Erlangen, Germany

† Electronic supplementary information (ESI) available: Gel Permeation Chromatography (GPC), 1H-NMR spectra, atmospheric pressure photoelectron spectroscopy graph of the studied material and external quantum efficiency graph. See DOI: 10.1039/c5ta04229a



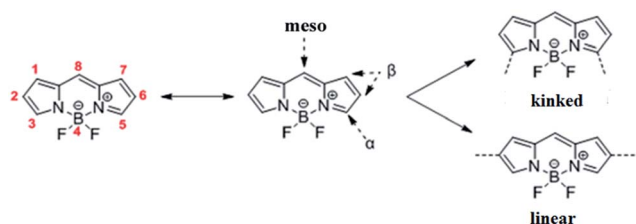
straightforward chemical synthesis and structural robustness have enabled fine tuning of optical properties of BODIPY dyes *via* systematic structural variations.<sup>23</sup> Owing to large extinction coefficients, intense absorption spectra that extend into the red region of the visible spectrum, and decent hole mobility, small-molecule BODIPY derivatives have been recently employed as p-type or donor materials in conjunction with PCBM in bulk heterojunction (BHJ) solar cells.<sup>25</sup>

Despite the fact that BODIPY-based conjugated polymers have also been used in different applications,<sup>26–35</sup> such as near-IR emitters, nonlinear optics, light harvesting, electrochromics and OPVs, limited examples have been presented up to now with ultra LBG conjugated polymers ( $E_g < 1.4–1.5$  eV) consisting of the BODIPY core. As a matter of fact, Algi and Cihaner<sup>32</sup> designed and synthesized a BODIPY-based polymer for electrochromic applications. In their study, a 1,3,5,7-tetramethyl substituted BODIPY derivative was used as an acceptor unit, featuring a non-planar repeating unit and distorted conjugation between EDOT (strong electron rich) and BODIPY (electron deficient) units due to the steric effect of the methyl groups. To avoid the steric effect of the methyl groups, Vobecka *et al.*<sup>33</sup> and Samuel *et al.*<sup>34</sup> have synthesized a BODIPY core with halogens at 3- and 5-positions ( $\alpha$ -positions; Scheme 1) and effectively synthesized an EDOT-BODIPY-EDOT conjugated polymer both with electropolymerization and Stille cross coupling polymerization, respectively. However, the resulting copolymers are kinked because the linearity of the polymer was lost (Scheme 1). Last year, Stoddart *et al.*<sup>36</sup> succeeded to synthesize the first ultra LBG DAD type  $\alpha,\beta$ -unsubstituted BODIPY-based copolymer using EDOT as the electron rich (D) unit by electropolymerization which displays electrochromic behavior.

In this work, it is presented for the first time the successful synthesis and optoelectronic characterization of an ultra LBG ( $E_g = 1.15$  eV) linear BODIPY-based copolymer by conventional cross coupling polymerization procedure (Stille cross coupling). The new synthesized NIR BODIPY copolymer exhibits a broad (panchromatic) absorption spectrum ranging from 300 nm to 1100 nm, while initial photovoltaic characterization as electron donor in BHJ OPVs reveals very interesting and promising photovoltaic characteristics such as good fill factor (FF) and open circuit voltage ( $V_{oc}$ ).

## 2. Results and discussion

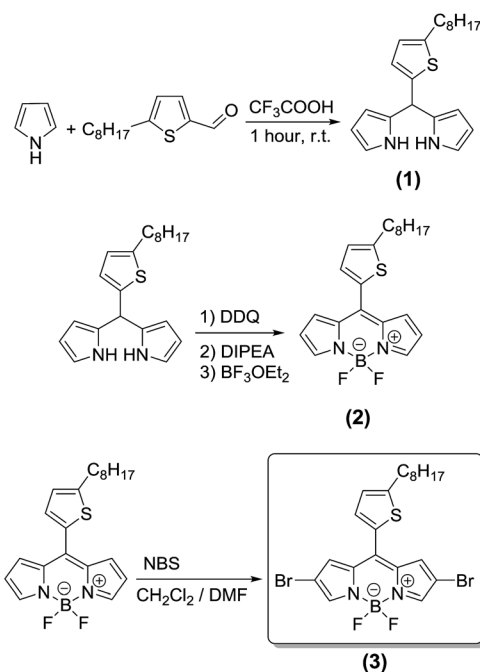
The preferred method of choice for the synthesis of  $\alpha,\beta$ -unsubstituted BODIPY dyes is the combination of aldehydes



Scheme 1 Chemical structure of BODIPY dye and assignment of the different positions and forms.

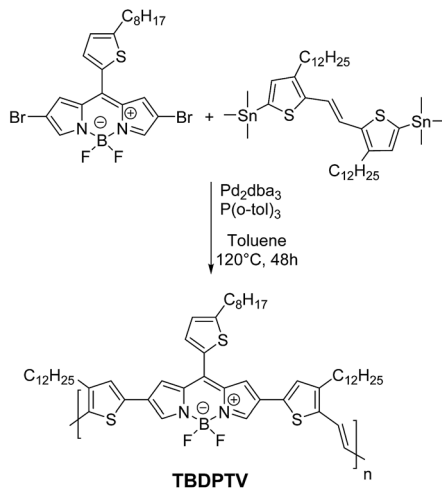
and pyrrole under neat conditions.<sup>23,37</sup> The aldehyde can be dissolved in excess pyrrole at room temperature, and the dipyrromethane intermediate (the reduced form of the dipyrromethene) is formed and isolated. The BODIPY core can then be obtained after oxidation and complexation with boron. In this work, 5-octylthiophene-2-carbaldehyde has been chosen as the aldehyde, where upon condensation with pyrrole, catalyzed by few drops of trifluoroacetic acid, the resulting 2,2'-((5-octylthiophen-2-yl)methylene)bis(1*H*-pyrrole) (1) is obtained (Scheme 2). The design concept of choosing an alkylthiophene-carbaldehyde is the formation of a functional BODIPY building block (3) with a 2D extension for the development of a series of BODIPY based copolymers soluble in common organic solvents. Treatment of monomer 1 with the strong oxidant 2,3-dichloro-5,6-dicyano-1,4-benzoquinone (DDQ), then diisopropylethylamine (Hünig's base) and finally with trifluoroborane dietherate [ $\text{BF}_3\text{O}(\text{Et})_2$ ] provided the corresponding borondipyrromethene monomer 2. Recently, new synthetic protocols to introduce bromine atoms at the 2- and 6-positions on the unsubstituted BODIPY core have been presented in the literature.<sup>38</sup> In our case, the targeted dibromo borondipyrromethene monomer 3 is synthesized upon bromination with *N*-bromosuccinimide (NBS) using dimethylformamide (DMF) : methylene chloride ( $\text{CH}_2\text{Cl}_2$ ) 1 : 1 as the solvent mixture similar to the conditions presented elsewhere.<sup>36,38c</sup>

For the synthesis of TBDPTV, Stille cross-coupling polymerization using 1 : 1 monomer feed ratios was used (Scheme 3). A solution of the commercially available (*E*)-1,2-bis(3-dodecyl-5-(trimethylstannyl)thiophen-2-yl)ethane and the dibromo borondipyrromethene monomer 3 were combined in dry deoxygenated toluene in the presence of tris(dibenzylideneacetone)



Scheme 2 Reaction procedures towards the synthesis of dibromo borondipyrromethene monomer 3.





**Scheme 3** Synthesis of TBDPTV by Stille cross coupling polymerization.

dipalladium(0) [ $\text{Pd}_2(\text{dba})_3$ ] (5 mol%) and tri-*o*-tolylphosphine [ $\text{P}(\text{o-Tol})_3$ ] (40 mol%) and the mixture was heated to *ca.* 120 °C for 48 h to provide the desired crude polymer. Purification was achieved by Soxhlet extraction with methanol (200 mL, 1 d), hexane (200 mL, 1 d) and chloroform (200 mL, 1 d). The chloroform fraction was then concentrated under reduced pressure, precipitated in methanol, filtered and dried in vacuum. The resulting TBDPTV is readily soluble in chloroform, chlorobenzene and *o*-dichlorobenzene (*o*-DCB). The polymer was characterized with  $^1\text{H}$  NMR spectroscopy and gel permeation chromatography (GPC) [see ESI (Fig. S1–S2†)]. The typical molecular weight characteristics of TBDPTV were estimated by GPC and presented in Table 1.

The normalized UV-vis absorption spectra of TBDPTV in chloroform solution and in the solid state are presented in Fig. 1, and the corresponding optical properties are summarized in Table 1.

Two major absorption bands can be observed in solution, a feature, which is commonly observed for alternating D-A copolymers. The low-wavelength peak observed at 444 nm for can be attributed to a  $\pi$ - $\pi^*$  transition, while the high-wavelength transition with maximum absorption at 817 nm is believed to be related to an intramolecular charge transfer (ICT) between the electron donor and the electron deficient of the repeating unit.

Passing from solution to the solid state, the absorption spectrum of TBDPTV becomes broader covering all the range from 300 nm to 1100 nm. All the absorption bands are red-

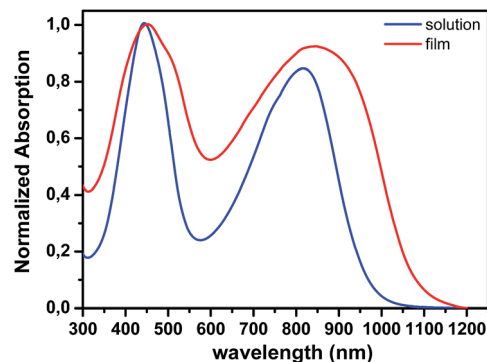


**Fig. 1** Absorption spectra of TBDPTV in chloroform solution and as thin film.

shifted when passing from solution to the solid state, the peak at 444 nm in solution is situated at 451 nm in the solid state whereas the peak at 817 nm in solution has been shifted to 848 nm in the solid state, indicating the presence of strong intermolecular  $\pi$ - $\pi$  interactions. The optical band gap ( $E_g^{\text{opt}}$ ) deduced from the absorption onset in the solid state is estimated at 1.15 eV.

The energy levels of TBDPTV have been determined utilizing both cyclic voltammetry (CV) and atmospheric pressure photoelectron spectroscopy (AAPPS, AC-2). TBDPTV exhibits reduction and oxidation peak potentials *versus* saturated calomel electrode (SCE) at  $-0.68$  V and  $0.46$  V, respectively as obtained by cyclic voltammetry (Fig. 2). The resulting HOMO ( $E_{\text{HOMO}}$ ) and LUMO ( $E_{\text{LUMO}}$ ) energy levels as derived from the equations

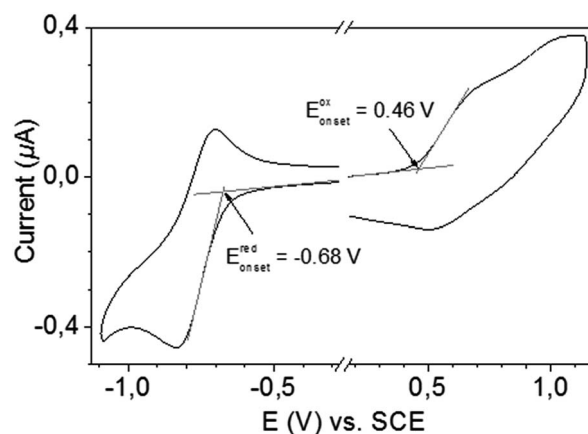


**Fig. 2** Cyclic voltammogram of TBDPTV in chloroform (containing 0.1 M tetrabutylammonium perchlorate).

**Table 1** Molecular weight characteristics, optical and electrochemical properties of TBDPTV

Polymer	$M_n$ (g mol $^{-1}$ )	$M_w$ (g mol $^{-1}$ )	$\lambda_{\text{max}}^{\text{sol}}$ (nm)	$\lambda_{\text{max}}^{\text{film}}$ (nm)	$E_g^{\text{opt}}$ (eV)	$E_{\text{HOMO}}^{\text{AAPPS}}$ (eV)	$E_{\text{HOMO}}^{\text{CV}}$ (eV)	$E_{\text{LUMO}}^{\text{CV}}$ (eV)
TBDPTV	13 700 (UV) 14 000 (RI)	70 300 (UV) 71 100 (RI)	444 817	451 848	1.15	$-5.29$	$-5.16$	$-4.02$



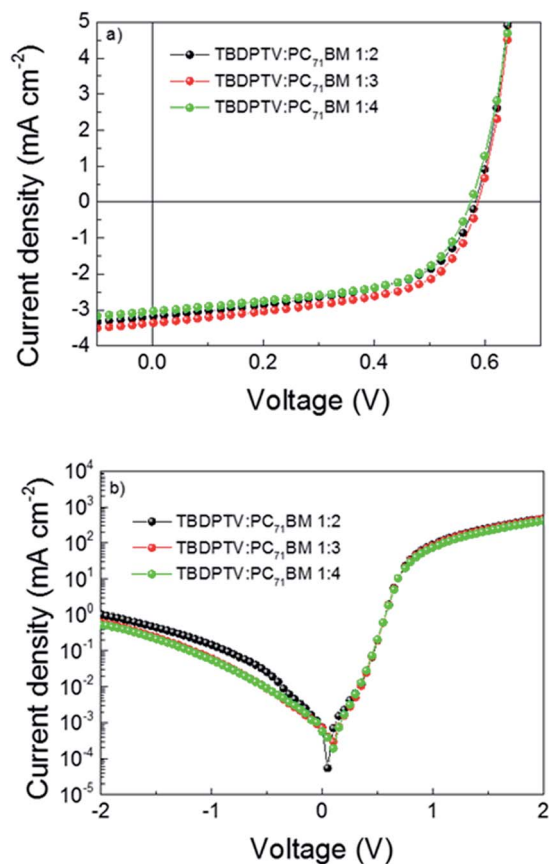


Fig. 3 Current density–voltage characteristics under  $100 \text{ mW cm}^{-2}$  illumination (AM 1.5G) (a) in linear graph and (b) in semilogarithmic graph.

$E_{\text{HOMO}} = -(4.7 + E_{\text{onset}}^{\text{ox}})$  eV and  $E_{\text{LUMO}} = -(4.7 + E_{\text{onset}}^{\text{red}})$  eV are  $-5.16$  eV and  $-4.02$  eV vs. vacuum, respectively. The electrochemical bandgap ( $E_{\text{g}}^{\text{CV}}$ ) of  $1.14$  eV is in excellent agreement with the  $E_{\text{g}}^{\text{opt}}$ . The HOMO level as calculated by AAPPs (Fig. S3 in ESI†) is situated at  $-5.29$  eV, slightly different from the one obtained by cyclic voltammetry.

An attempt to probe the photovoltaic properties of the synthesized polymer was carried out. Organic BHJ solar cells were fabricated in inverted device structure consisting of ITO/ZnO/TBDPTV:PC<sub>71</sub>B/MoO<sub>x</sub>/Ag, using the three different D:A composition ratio (1:2, 1:3 and 1:4). The active layer solution was spin coated under inert atmosphere condition using 97 to 3 vol% of chlorobenzene (CB) and 1,8 diiodooctane (DIO). Fig. 3a and b show the  $J$ - $V$  curves of the optimized BHJ solar cells under simulated AM 1.5G solar irradiance ( $100 \text{ mW}$

$\text{cm}^{-2}$ ) and in the dark, respectively. A PCE of 1.1% was obtained for the 1:3 ratio, with a short circuit current density ( $J_{\text{sc}}$ ) of  $3.39 \text{ mA cm}^{-2}$ ,  $V_{\text{oc}}$  of  $0.59 \text{ V}$  and FF of 0.56. Using the same fabrication conditions, solar cells containing 1:2 and 1:4 D:A ratio achieved a maximum efficiency of 1.03 and 1.01, respectively. A strong correlation between the charge carrier mobility and FFs is also obtained for these devices. In fact, as shown in Table 2, solar cells based on 1:3 and 1:4 ratio, display the highest FF of 0.56 and 0.57, respectively. On the other hand, the 1:2 based devices depicted a lower FF of 0.52, costing with the lower charge carrier mobility obtained. It is worth to mention that for all the devices,  $J_{\text{sc}}$  values are similar and this can be possible attributed to the not perfect energy alignment with PC<sub>71</sub>B for achieving efficient exciton splitting rather than to morphological issues as can be seen on Fig. 5. Furthermore, external quantum efficiency (EQE) measurements have been carried out (Fig. S4†). An EQE signal around 950–1000 nm, even though very weak, is observed, suggesting an existing path towards charge generation from the polymer. As reported by Janssen *et al.*,<sup>39</sup> a fast recombination path becomes essential when the LUMO of the acceptor become too shallow, leading to low  $J_{\text{sc}}$  values. Noticeably, the rectification behavior of the device slightly improved with increasing the D:A ratio (Fig. 3b). The  $J_{\text{sc}}$  calculated from the EQE is  $3.08 \text{ mA cm}^{-3}$ , which is less than 10% smaller compared to the  $J_{\text{sc}}$  obtained from the solar simulator.

In order to understand the transport properties of TBDPTV-based solar cells, the charge carrier mobility  $\mu$  of the aforementioned devices were determined by employing the technique of photoinduced charge carrier extraction by linearly increasing voltage (photo-CELIV).<sup>40</sup> Charges are photogenerated by a strongly absorbed laser pulse and extracted after an adjustable delay time. Fig. 4 shows the photo-CELIV transients of the TBDPTV:PC<sub>71</sub>B system in the three different composition ratio (1:2, 1:3 and 1:4), which were recorded by applying a  $2 \text{ V}/20 \mu\text{s}$  linearly increasing reverse bias pulse and a delay time ( $t_{\text{d}}$ ) of  $1 \mu\text{s}$ . From the measured photocurrent transients, the charge carrier mobility ( $\mu$ ) is calculated using the following equation:

$$\mu = \frac{2d^2}{3At_{\text{max}}^2 \left[ 1 + 0.36 \frac{\Delta j}{j(0)} \right]} \quad \text{if } \Delta j \leq j(0)$$

where  $d$  is the active layer thickness,  $A$  is the voltage rise speed  $dU/dt$ ,  $U$  is the applied voltage,  $t_{\text{max}}$  is the time corresponding to the maximum of the extraction peak, and  $j(0)$  is the displacement current.<sup>41</sup> The photocurrent transients in Fig. 4 reveal that

Table 2 Photovoltaic parameters of TBDPTV:PC<sub>71</sub>B system in different composition ratio

TBDPTV:PC <sub>71</sub> B	$V_{\text{oc}}$ [V]	$J_{\text{sc}}$ [ $\text{mA cm}^{-2}$ ]	FF [%]	$\eta$ [%]
1:2	0.58 (0.58 ± 0.00)	3.32 (3.27 ± 0.32)	53.45 (51.54 ± 1.82)	1.03 (0.97 ± 0.04)
1:3	0.59 (0.59 ± 0.00)	3.39 (3.16 ± 0.17)	56.18 (55.52 ± 0.58)	1.10 (1.03 ± 0.06)
1:4	0.59 (0.59 ± 0.00)	3.12 (2.86 ± 0.24)	56.51 (56.14 ± 0.37)	1.01 (0.93 ± 0.07)



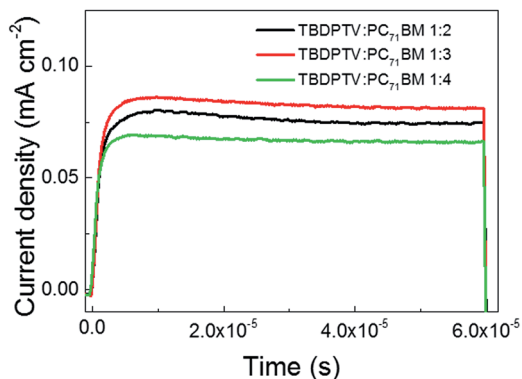


Fig. 4 Time-dependent photo-CELIV traces of TBDPTV-based solar cells at a fixed delay time of  $1 \mu\text{s}$ .

$t_{\text{max}}$  occurs significantly earlier for the 1 : 4 weight ratio. As a result, the calculated charge carrier mobility ( $\mu$ ) is higher for the 1 : 4 ratio  $(1.05 \pm 0.2) \times 10^{-5} \text{ cm}^2 \text{ V}^{-1} \text{ s}^{-1}$ , then for the 1 : 3 ratio  $(9.18 \pm 0.2) \times 10^{-6} \text{ cm}^2 \text{ V}^{-1} \text{ s}^{-1}$ , and finally for the 1 : 2 ratio  $(7.50 \pm 0.1) \times 10^{-6} \text{ cm}^2 \text{ V}^{-1} \text{ s}^{-1}$ , respectively.

Investigations on the surface microstructure were also carried out through intermittent contact mode atomic force microscopy (AFM, Fig. 5). A good intermixing between the donor and the acceptor materials is obtained, consequentially the topography and the phase images do not reveal obvious differences between the three systems studied, supporting the hypothesis that the main limitations on TBDPTV-based solar cells are attributed to the low LUMO offset rather than to morphological issues.

### 3. Conclusions

A dibromo  $\alpha,\beta$ -unsubstituted BODIPY building block suitable for conventional catalyzed cross coupling polymerizations has been effectively synthesized. In order to confirm the proof of concept, the dibromo BODIPY monomer 3 has been successfully polymerized through Stille cross coupling with (*E*)-1,2-bis(3-dodecyl-5-(trimethylstannyl)thiophen-2-yl)ethane as the comonomer providing the new ultra LBG ( $E_{\text{g}}^{\text{opt}} = 1.15 \text{ eV}$ ) TBDPTV copolymer. To the best of our knowledge TBDPTV is the first  $\alpha,\beta$ -unsubstituted BODIPY-based NIR copolymer synthesized by conventional catalyzed cross coupling polymerization methods. TBDPTV exhibits a panchromatic absorption spectrum ranging from 300 nm to 1100 nm, and a promising PCE of 1.1% in NIR BHJ OPVs using PC<sub>71</sub>BM as the electron acceptor with very interesting photovoltaic characteristics, such as good fill factor (FF) and open circuit voltage ( $V_{\text{oc}}$ ).

### 4. Experimental

All reactions were treated as air and light sensitive and performed under argon and in the dark. All glassware used were washed using teepol surfactant, rinsing with excess water, acetone and methylene dichloride and dried in an oven at  $120 \text{ }^\circ\text{C}$ . All solvents and reagents were sourced commercially from Aldrich, except (*E*)-1,2-bis(3-dodecyl-5-(trimethylstannyl)thiophen-2-yl)ethane which was obtained from Solarmer Materials Inc.

#### Synthetic procedures

**2,2'-((5-octylthiophen-2-yl)methylene)bis(1*H*-pyrrole) 1.** 5-Octylthiophene-2-carbaldehyde (2.24 g, 10 mmol) was dissolved

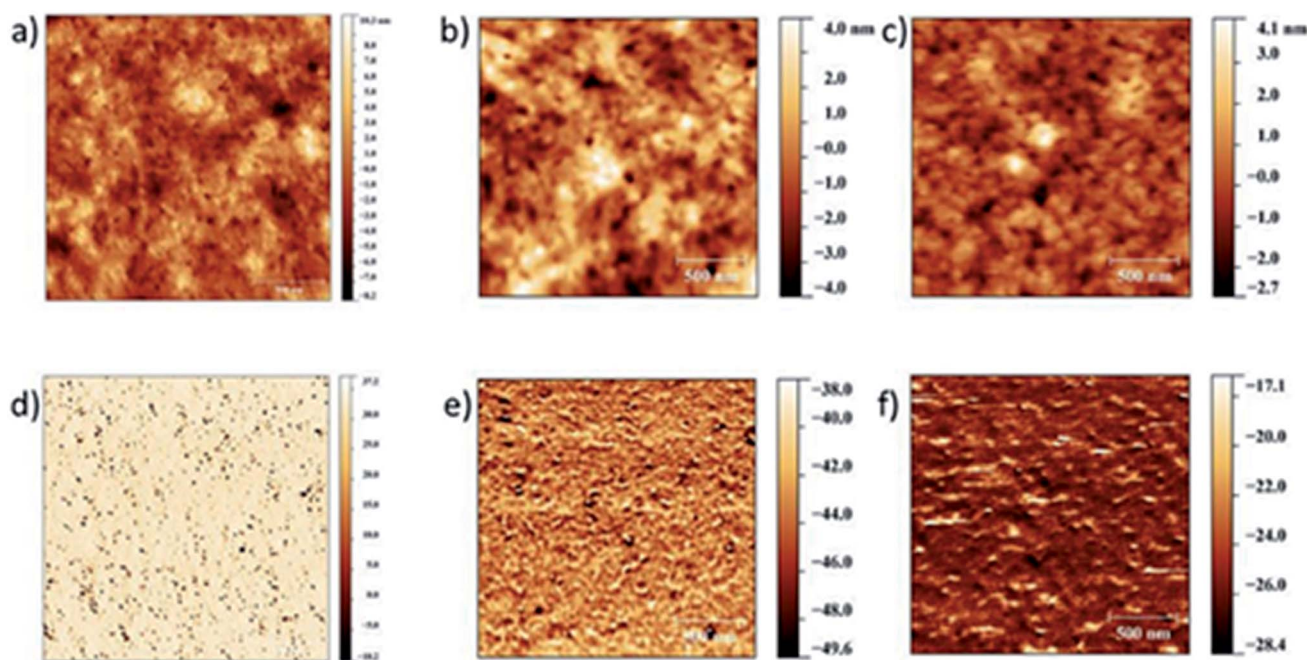


Fig. 5 Topography (a, b and c) and phase (d, e and f) images of films TBDPTV : PC<sub>71</sub>BM 1 : 2, 1 : 3 and 1 : 4 respectively, on top of a layer of ZnO, as measured by intermittent contact mode atomic force microscopy.



in excess of pyrrole (28 mL, 400 mmol). The resulting mixture was degassed for 30 min by argon and then 0.1 mL of trifluoroacetic acid were added. The reaction was stirred at room temperature for an hour and the crude product was diluted with methylene chloride and washed three times with sodium hydroxide (NaOH) aq. 0.1 N and dried on magnesium sulphate. The solvent was removed under reduced pressure. The product was purified by chromatography on silica gel using hexane/ethyl acetate 9 : 1 as eluent. The yellow-green oil product obtained with a yield of 71% (2.40 g).

$^1\text{H}$  NMR ( $\text{CDCl}_3$ , 400 MHz):  $\delta$  8.0 (s, 2H), 6.70 (dd,  $^3J = 6.70$  Hz, 2H), 6.60 (d, 1H), 6.17 (dd,  $^3J = 6.17$  Hz, 2H), 6.04 (s, 2H), 5.66 (s, 1H), 2.73 (t, 2H), 1.63 (m, 2H), 1.29 (m, 10H), 0.89 (t, 3H).

**Borondipyrromethene monomer 2.** Monomer 1 (2.30 g, 6.8 mmol) and the DDQ (1.57 g, 6.8 mmol) were dissolved in dry toluene (70 mL) and then added in a predegassed three necked flask. After 30 min the predistilled Hünig's base (DIPEA, 5.6 mL) was added and the mixture stirred at room temperature for 90 min. Finally the boron trifluoride diethyl etherate (5.7 mL) was added and the mixture was stirred at 80 °C for 2 h and then cooled at room temperature. The crude product was washed with water and dried on magnesium sulphate. The solvent was removed under reduced pressure and the product was purified by silica gel chromatography using a mixture of dichloromethane : hexane 2 : 1 as eluent. The product obtained as a red-orange oil with a yield of 40% (1.43 g).

$^1\text{H}$  NMR ( $\text{CDCl}_3$ , 400 MHz):  $\delta$  7.9 (s, 2H), 7.44 (d,  $J = 3.6$  Hz, 2H), 7.32 (d,  $J = 3.6$  Hz, 2H), 6.97 (d,  $J = 3.2$  Hz, 1H), 6.57 (m, 2H), 2.92 (t,  $J = 7.6$  Hz, 2H), 1.76 (m, 2H), 1.29 (m, 10H), 0.89 (t,  $J = 6.8$  Hz, 3H).

$^{13}\text{C}$  NMR ( $\text{CDCl}_3$ , 100 MHz):  $\delta$  154.21, 143.11, 133.79, 132.13, 131.30, 125.88, 118.19, 31.83, 31.49, 29.26, 28.18, 22.85, 14.19, 0.99.

**Dibromo-borondipyrromethene monomer 3.** To a solution of BODIPY monomer 2 (0.200 g, 0.52 mmol) in methylene chloride (13 mL) and dimethylformamide (13 mL) was added portion-wise *N*-bromosuccinimide (0.222 g) at room temperature. The mixture was stirred at room temperature for 2 h. The crude product was diluted in methylene chloride and washed with brine 3 times. The organic phase was dried on magnesium sulphate and the solvent was removed under reduced pressure. The product was purified by silica-gel column chromatography using hexane as eluent and then increasing slowly the polarity to 7 : 3 hexane/methylene chloride. The product obtained as a pink solid with yield of 50% (0.120 g).

$^1\text{H}$  NMR ( $\text{CDCl}_3$ , 400 MHz):  $\delta$  7.8 (s, 2H), 7.48 (d,  $J = 3.7$  Hz, 1H), 7.32 (s, 2H), 7.0 (d,  $J = 3.6$  Hz, 1H), 2.93 (t,  $J = 7.7$  Hz, 2H), 1.77 (m, 2H), 1.38 (m, 10H), 0.89 (t,  $J = 6.4$  Hz, 3H).

$^{13}\text{C}$  NMR ( $\text{CDCl}_3$ , 100 MHz):  $\delta$  156.36, 142.84, 135.02, 131.40, 126.61, 31.83, 31.46, 30.55, 29.24, 29.17, 22.65, 14.11.

MALDI *m/z*, calcd for  $\text{C}_{21}\text{H}_{23}\text{BBr}_2\text{F}_2\text{N}_2\text{S}$  ( $\text{M}^+$ ): 543.10; found: 543.14.

### Synthesis of TBDPTV

Dibromo-BODIPY monomer 3 (0.2022 mmol, 110 mg) and the distannyl-derivative (0.2022 mmol, 172.8 mg) were dissolved in

dry toluene (8.1 mL). Then,  $\text{Pd}_2\text{dba}_3$  (0.0101 mmol, 9.3 mg) and  $\text{P}(o\text{-tol})_3$  (0.0808 mmol, 24.6 mg) were added and the reaction mixture was stirred at 120 °C under argon atmosphere for 48 h. Then, the toluene solution was evaporated, the mixture was solubilized in  $\text{CHCl}_3$ . The polymer was purified by precipitation in methanol, filtered and washed on Soxhlet apparatus with methanol, hexane and chloroform. The chloroform fraction was evaporated under reduced pressure and the polymer was precipitated in acetone, filtered and finally dried under high vacuum, providing a greenish solid (52 mg).

### Instrumentation and materials characterization

**Nuclear magnetic resonance (NMR).**  $^1\text{H}$  and  $^{13}\text{C}$  NMR spectra were recorded on a Bruker AV-400 (400 MHz for  $^1\text{H}$  and 100 MHz for  $^{13}\text{C}$ ), using the residual solvent resonance of  $\text{CDCl}_3$  as an internal reference.

**Gel permeation chromatography (GPC).**  $M_n$  and  $M_w$  of the polymer have been determined by GPC on a PSS/Agilent SECurity GPC system, equipped with two PSS SDV analytical linear M columns, ALSG1329A DAD detector, and RID G1362A RI detector. The measurement was performed with chloroform as eluent, with a sample concentration of 0.8 g  $\text{L}^{-1}$ .

**Absorption spectroscopy.** UV/vis spectra were measured on a Jasco V-670 spectrophotometer.

**Cyclic voltammetry.** Cyclic voltammetry was executed in chloroform with 0.1 M (*n*-Bu) $_4\text{NClO}_4$  against standard calomel electrode. HOMO and LUMO levels were calculated using the formulae  $\text{HOMO} = -(E_{\text{ox}} + 4.7)$  eV and  $\text{LUMO} = -(E_{\text{red}} + 4.7)$  eV, respectively. The potentiostat was a PAR VersaSTAT4 and the working electrode used is platinum.

**Atmospheric pressure photoelectron spectroscopy.** AAPPs has been performed on a Riken Keiki AC-2 spectrometer in thin film at room temperature.

**Fabrication of photovoltaic devices.** All devices were fabricated using doctor-blading under ambient conditions. Pre-structured indium tin oxide (ITO) substrates were cleaned with acetone and isopropyl alcohol in an ultrasonic bath for 10 minutes each. After drying, the substrates were successively coated with 40 nm of zinc oxide (ZnO), 10 nm of  $\text{Ba}(\text{OH})_2$  and finally a 80–90 nm thick active layer based on TBDPTV :  $\text{PC}_{70}\text{BM}$  (20 g  $\text{L}^{-1}$ ). To complete the fabrication of the devices 10 nm of MoOx and 100 nm of Ag were thermally evaporated through a mask (with a 10.4  $\text{mm}^2$  active area opening) under a vacuum of  $\sim 5 \times 10^{-6}$  mbar.

***J*-*V* measurements.** The *J*-*V* characteristics was measured using a source measurement unit from BoTest. Illumination was provided by a solar simulator (Oriel Sol 1A, from Newport) with AM 1.5G spectrum at 100  $\text{mW cm}^{-2}$ . EQEs were measured using an integrated system from Enlitech, Taiwan. In order to study the light intensity dependence of current density, we used a series of neutral color density filters. The intensity of light transmitted through the filter was independently measured *via* a power meter. All the devices were tested in ambient air.

**Photo-CELIV.** In photo-CELIV measurements, the devices were illuminated with a 405 nm laser-diode. Current transients were recorded across an internal 50  $\Omega$  resistor of an oscilloscope



(Agilent Technologies DSO-X 2024A). We used a fast electrical switch to isolate the cell and prevent charge extraction or sweep out during the laser pulse and the delay time. After a variable delay time, a linear extraction ramp is applied *via* a function generator. The ramp, which was 20  $\mu\text{s}$  long and 2 V in amplitude, was set to start with an offset matching the  $V_{oc}$  of the cell for each delay time.

**Atomic force microscopy.** AFM measurements were performed on a solver nano from NT-MDT using 300 kHz single crystal silicon cantilevers (NT-MDT, NSG30).

## Acknowledgements

This project has received funding from the European Community's Seventh Framework Programme (FP7/2007–2013) under the Grant Agreement no. 607585. The authors acknowledge the financial support of a Marie Curie Initial Training Network (FP7-PEOPLE-2013-ITN) project OSNIRO. The authors thank Anke Helfer and Sylwia Adamczyk for performing the GPC- and PESA measurements.

## Notes and references

- G. Qian and Z. Y. Wang, *Chem.-Asian J.*, 2010, 5, 1006.
- A. J. Heeger, *Adv. Mater.*, 2014, 26, 10.
- (a) J. D. Yuen, R. Kumar, D. Zakhidov, J. Seifert, B. Lim, A. J. Heeger and F. Wudl, *Adv. Mater.*, 2011, 23, 3780; (b) J. Fan, J. D. Yuen, M. Wang, J. Seifert, J.-H. Seo, A. R. Mohebbi, D. Zakhidov, A. Heeger and F. Wudl, *Adv. Mater.*, 2012, 24, 2186; (c) J. D. Yuen, J. Fan, J. Seifert, B. Lim, R. Hufschmid, A. J. Heeger and F. Wudl, *J. Am. Chem. Soc.*, 2011, 133, 20799; (d) C. Yang, S. Cho, R. C. Chiechi, W. Walker, N. E. Coates, D. Moses, A. J. Heeger and F. Wudl, *J. Am. Chem. Soc.*, 2008, 130, 16524; (e) W. Cui and F. Wudl, *Macromolecules*, 2013, 46, 7232; (f) A. R. Mohebbi, J. Yuen, J. Fan, C. Munoz, M. F. Wang, R. S. Shirazi, J. Seifert and F. Wudl, *Adv. Mater.*, 2011, 23, 4644; (g) J. D. Yuen and F. Wudl, *Energy Environ. Sci.*, 2013, 6, 392.
- (a) M. M. Wienk, M. G. R. Turbiez, M. P. Struijk, M. Fonrodona and R. A. J. Janssen, *Appl. Phys. Lett.*, 2006, 88, 153511; (b) G. W. P. van Pruijsen, F. Gholamrezaie, M. M. Wienk and R. A. J. Janssen, *J. Mater. Chem.*, 2012, 22, 20387; (c) K. H. Hendriks, W. Li, M. M. Wienk and R. A. J. Janssen, *J. Am. Chem. Soc.*, 2014, 136, 12130; (d) A. P. Zoombelt, M. Fonrodona, M. M. Wienk, A. B. Sieval, J. C. Hummelen and R. A. J. Janssen, *Org. Lett.*, 2009, 11, 903.
- (a) Y. Yao, Y. Liang, V. Shrotriya, S. Xiao, L. Yu and Y. Yang, *Adv. Mater.*, 2007, 19, 3979; (b) L. Dou, C.-C. Chen, K. Yoshimura, K. Ohya, W.-H. Chang, J. Gao, Y. Liu, E. Richard and Y. Yang, *Macromolecules*, 2013, 46, 3384; (c) L. Dou, W.-H. Chang, J. Gao, C.-C. Chen, J. You and Y. Yang, *Adv. Mater.*, 2013, 25, 825.
- Y. Xia, L. Wang, X. Deng, D. Li, X. Zhu and Y. Cao, *Appl. Phys. Lett.*, 2006, 89, 081106.
- (a) P. M. Beaujuge, S. Ellinger and J. R. Reynolds, *Nat. Mater.*, 2008, 7, 795; (b) T. T. Steckler, X. Zhang, J. Hwang, R. Honeyager, S. Ohira, X.-H. Zhang, A. Grant, S. Ellinger, S. A. Odom, D. Sweat, D. B. Tanner, A. G. Rinzler, S. Barlow, J.-L. Brédas, B. Kippelen, S. R. Marder and J. R. Reynolds, *J. Am. Chem. Soc.*, 2009, 131, 2824.
- (a) P.-T. Wu, F. S. Kim and S. A. Jenekhe, *Chem. Mater.*, 2011, 23, 4618; (b) H. Li, F. S. Kim, G. Ren and S. A. Jenekhe, *J. Am. Chem. Soc.*, 2013, 135, 14920; (c) H. Li, Y.-J. Hwang, T. Earmme, R. C. Huber, B. A. E. Courtright, C. O'Brien, S. H. Tolbert and S. A. Jenekhe, *Macromolecules*, 2015, 48, 1759; (d) Y.-J. Hwang, F. S. Kim, H. Xin and S. A. Jenekhe, *Macromolecules*, 2012, 45, 3732.
- (a) T. T. Steckler, P. Henriksson, S. Mollinger, A. Lundin, A. Salleo and M. R. Andersson, *J. Am. Chem. Soc.*, 2014, 136, 1190; (b) E. Wang, L. Hou, Z. Wang, S. Hellström, W. Mammo, F. Zhang, O. Inganäs and M. R. Andersson, *Org. Lett.*, 2010, 12, 4470.
- (a) T. L. D. Tam, T. Salim, H. Li, F. Zhou, S. G. Mhaisalkar, H. Su, Y. M. Lam and A. C. Grimsdale, *J. Mater. Chem.*, 2012, 22, 18528; (b) T. L. D. Tam, W. Ye, H. H. R. Tan, F. Zhou, H. Su, S. G. Mhaisalkar and A. C. Grimsdale, *J. Org. Chem.*, 2012, 77, 10035.
- (a) M. Li, C. An, T. Marszalek, X. Guo, Y.-Z. Long, H. Yin, C. Gu, M. Baumgarten, W. Pisula and K. Müllen, *Chem. Mater.*, 2015, 27, 2218; (b) T. Dallos, D. Beckmann, G. Brunklaus and M. Baumgarten, *J. Am. Chem. Soc.*, 2011, 133, 13898; (c) C. An, S. R. Puniredd, X. Guo, T. Stelzig, Y. Zhao, W. Pisula and M. Baumgarten, *Macromolecules*, 2014, 47, 979.
- (a) H. Usta, C. Newman, Z. Chen and A. Facchetti, *Adv. Mater.*, 2012, 24, 3678; (b) H. Huang, Z. Chen, R. P. Ortiz, C. Newman, H. Usta, S. Lou, J. Youn, Y.-Y. Noh, K.-J. Baeg, L. X. Chen, A. Facchetti and T. Marks, *J. Am. Chem. Soc.*, 2012, 134, 10966.
- (a) R. S. Ashraf, I. Meager, M. Nikolka, M. Kirkus, M. Planells, B. C. Schroeder, S. Holliday, M. Hurhangee, C. B. Nielsen, H. Sirringhaus and I. McCulloch, *J. Am. Chem. Soc.*, 2015, 137, 1314; (b) R. S. Ashraf, A. J. Kronemeijer, D. I. James, H. Sirringhaus and I. McCulloch, *Chem. Commun.*, 2012, 48, 3939; (c) H. Bronstein, E. Collado-Fregoso, A. Hadipour, Y. W. Soon, Z. Huang, S. D. Dimitrov, R. S. Ashraf, B. P. Rand, S. E. Watkins, P. S. Tuladhar, I. Meager, J. R. Durrant and I. McCulloch, *Adv. Funct. Mater.*, 2013, 23, 5647; (d) I. Meager, M. Nikolka, B. C. Schroeder, C. B. Nielsen, M. Planells, H. Bronstein, J. W. Rumer, D. I. James, R. S. Ashraf, A. Sadhanala, P. Hayoz, J.-C. Flores, H. Sirringhaus and I. McCulloch, *Adv. Funct. Mater.*, 2014, 24, 7109; (e) J. W. Rumer, M. Levick, S.-Y. Dai, S. Rossbauer, Z. Huang, L. Biniak, T. D. Anthopoulos, J. R. Durrant, D. J. Procter and I. McCulloch, *Chem. Commun.*, 2013, 49, 4465; (f) H. Bronstein, Z. Chen, R. S. Ashraf, W. Zhang, J. Du, J. R. Durrant, P. S. Tuladhar, K. Song, S. E. Watkins, Y. Geerts, M. M. Wienk, R. A. J. Janssen, T. Anthopoulos, H. Sirringhaus, M. Heeney and I. McCulloch, *J. Am. Chem. Soc.*, 2011, 133, 3272.



- 14 (a) Z. Fei, X. Gao, J. Smith, P. Pattanasattayavong, E. B. Domingo, N. Stingelin, S. E. Watkins, T. D. Anthopoulos, R. J. Kline and M. Heaney, *Chem. Mater.*, 2013, **25**, 59; (b) M. Shahid, T. McCarthy-Ward, J. Labram, S. Rossbauer, E. B. Domingo, S. E. Watkins, N. Stingelin, T. D. Anthopoulos and M. Heaney, *Chem. Sci.*, 2012, **3**, 181; (c) A. J. Kronemeijer, E. Gili, M. Shahid, J. Rivnay, A. Salleo, M. Heaney and H. Sirringhaus, *Adv. Mater.*, 2012, **24**, 1558.
- 15 (a) C. P. Yau, Z. Fei, R. S. Ashraf, M. Shahid, S. E. Watkins, P. Pattanasattayavong, T. D. Anthopoulos, V. G. Gregoriou, C. L. Chochos and M. Heaney, *Adv. Funct. Mater.*, 2014, **24**, 678; (b) C. L. Chochos, J. K. Kallitsis, P. E. Keivanidis, S. Balushev and V. G. Gregoriou, *J. Phys. Chem. B*, 2006, **110**, 4657.
- 16 (a) S. Cho, J. Lee, M. Tong, J. H. Seo and C. Yang, *Adv. Funct. Mater.*, 2011, **21**, 1910; (b) P. Sonar, S. P. Singh, Y. Li, M. S. Soh and A. Dodabalapur, *Adv. Mater.*, 2010, **22**, 5409.
- 17 (a) C. V. Hoven, X.-D. Dang, R. C. Coffin, J. Peet, T.-Q. Nguyen and G. C. Bazan, *Adv. Mater.*, 2010, **22**, E63; (b) G. C. Welch and G. C. Bazan, *J. Am. Chem. Soc.*, 2011, **133**, 4632; (c) L. Ying, B. B. Y. Hsu, H. Zhan, G. C. Welch, P. Zalar, L. A. Perez, E. J. Kramer, T.-Q. Nguyen, A. J. Heeger, W.-Y. Wong and G. C. Bazan, *J. Am. Chem. Soc.*, 2011, **133**, 18538.
- 18 (a) Z. Cai, H. Luo, P. Qi, J. Wang, G. Zhang, Z. Liu and D. Zhang, *Macromolecules*, 2014, **47**, 2899; (b) M. Karakawa and Y. Aso, *Macromol. Chem. Phys.*, 2013, **214**, 2388.
- 19 (a) R. Tautz, E. Da Como, T. Limmer, J. Feldmann, H.-J. Egelhaaf, E. von Hauff, V. Lemaur, D. Beljonne, S. Yilmaz, I. Dumsch, S. Allard and U. Scherf, *Nat. Commun.*, 2012, **3**, 970; (b) H. Reisch, U. Wiesler, U. Scherf and N. Tutyuykov, *Macromolecules*, 1996, **29**, 8204; (c) C. J. Kudla, D. Dolfen, K. J. Schottler, J.-M. Koenen, D. Breusov, S. Allard and U. Scherf, *Macromolecules*, 2010, **43**, 7864.
- 20 (a) C. L. Chochos and S. A. Choulis, *Prog. Polym. Sci.*, 2011, **36**, 1326; (b) J. Roncali, *Macromol. Rapid Commun.*, 2007, **28**, 1761.
- 21 (a) P.-L. T. Boudreault, A. Najari and M. Leclerc, *Chem. Mater.*, 2011, **23**, 456; (b) X. Guo, M. Baumgarten and K. Müllen, *Prog. Polym. Sci.*, 2013, **38**, 1832; (c) A. Facchetti, *Chem. Mater.*, 2011, **23**, 733.
- 22 C. L. Chochos, N. Tagmatarchis and V. G. Gregoriou, *RSC Adv.*, 2013, **3**, 7160.
- 23 (a) G. Ulrich, R. Ziesel and A. Harriman, *Angew. Chem., Int. Ed.*, 2008, **47**, 1184; (b) A. Loudet and K. Burgess, *Chem. Rev.*, 2007, **107**, 4891; (c) M. Benstead, G. H. Mehl and R. W. Boyle, *Tetrahedron*, 2011, **67**, 3573.
- 24 A. Treibs and F. H. Kreuzer, *Justus Liebig's Ann. Chem.*, 1968, **718**, 208.
- 25 (a) C. Qin, A. Mirloup, N. Leclerc, A. Islam, A. El-Shafei, L. Han and R. Ziesel, *Adv. Energy Mater.*, 2014, **4**, 1400085; (b) T. Rousseau, A. Cravino, T. Bura, G. Ulrich, R. Ziesel and J. Roncali, *Chem. Commun.*, 2009, 1673.
- 26 S. P. Economopoulos, C. L. Chochos, H. A. Ioannidou, M. Neophytou, C. Charilaou, G. A. Zissimou, J. M. Frost, T. Sachtan, M. Shahid, J. Nelson, M. Heaney, D. D. C. Bradley, G. Itskos, P. A. Koutentis and S. A. Choulis, *RSC Adv.*, 2013, **3**, 10221.
- 27 (a) B. Kim, B. W. Ma, V. R. Donuru, H. Y. Liu and J. M. J. Fréchet, *Chem. Commun.*, 2010, **46**, 4148; (b) R. Yoshii, H. Yamane, K. Tanaka and Y. Chujo, *Macromolecules*, 2014, **47**, 3755.
- 28 B. C. Popere, A. M. Della Pelle and S. Thayumanavan, *Macromolecules*, 2011, **44**, 4767.
- 29 (a) C. Thivierge, A. Loudet and K. Burgess, *Macromolecules*, 2011, **44**, 4012; (b) A. B. Nepomnyashchii, M. Bröring, J. Ahrens and A. J. Bard, *J. Am. Chem. Soc.*, 2011, **133**, 8633.
- 30 M. Zhu, L. Jiang, M. J. Yuan, X. F. Liu, C. B. Ouyang, H. Y. Zheng, X. D. Yin, Z. C. Zuo, H. B. Liu and Y. L. Li, *J. Polym. Sci., Part A: Polym. Chem.*, 2008, **46**, 7401.
- 31 S. L. Zhu, N. Dorh, J. T. Zhang, G. Vegesna, H. H. Li, F. T. Luo, A. Tiwari and H. Y. Liu, *J. Mater. Chem.*, 2012, **22**, 2781.
- 32 F. Algi and A. Cihaner, *Org. Electron.*, 2009, **10**, 453.
- 33 J. C. Forgie, P. J. Skabara, I. Stibor, F. Vilela and Z. Vobecka, *Chem. Mater.*, 2009, **21**, 1784.
- 34 D. Cortizo-Lacalle, C. T. Howells, S. Gambino, F. Vilela, Z. Vobecka, N. J. Findlay, A. R. Inigo, S. A. J. Thomson, P. J. Skabara and I. D. W. Samuel, *J. Mater. Chem.*, 2012, **22**, 14119.
- 35 H. Usta, M. D. Yilmaz, A.-J. Avestro, D. Boudinet, M. Denti, W. Zhao, J. F. Stoddart and A. Facchetti, *Adv. Mater.*, 2013, **25**, 4327.
- 36 M. D. Yilmaz, T. Aytun, M. Frasconi, S. I. Stupp and F. Stoddart, *Synth. Met.*, 2014, **197**, 52.
- 37 R. W. Wagner and J. S. Lindsey, *Pure Appl. Chem.*, 1996, **68**, 1373.
- 38 (a) L. Wang, J.-W. Wang, A.-J. Cui, X.-X. Cai, Y. Wan, Q. Chen, M.-Y. He and W. Zhang, *RSC Adv.*, 2013, **3**, 9219; (b) L. Jiao, W. Pang, J. Zhou, Y. Wei, X. Mu, G. Bai and E. Hao, *J. Org. Chem.*, 2011, **76**, 9988; (c) Y. Hayashi, S. Yamaguchi, W. Y. Cha, D. Kim and H. Shinokubo, *Org. Lett.*, 2011, **13**, 2992.
- 39 D. D. Nuzzo, G.-J. A. H. Wetzelaer, R. K. M. Bouwer, V. S. Gevaerts, S. C. J. Meskers, J. C. Hummelen, P. W. M. Blom and R. A. J. Janssen, *Adv. Energy Mater.*, 2013, **3**, 85.
- 40 G. J. R. O. A. Pivrikas and N. S. Sariciftci, *Progress in Photovoltaics: Research and Applications*, 2007, **15**, 677.
- 41 A. Mozer, G. Dennler, N. Sariciftci, M. Westerling, A. Pivrikas, R. Österbacka and G. Juška, *Phys. Rev. B: Condens. Matter Mater. Phys.*, 2005, **72**, 035217.

